



NUMERICAL SIMULATIONS OF THE VORTEX BREAKDOWN PHENOMENON

Diego Alves de Moro Martins

School of Mechanical Engineering, Federal University of Uberlandia.
Av. João Naves de Ávila, 2121, Uberlandia, Minas Gerais, Brazil.
moromartins@gmail.com

Francisco José de Souza

School of Mechanical Engineering, Federal University of Uberlandia.
Av. João Naves de Ávila, 2121, Uberlandia, Minas Gerais, Brazil.
fjsouza@mecanica.ufu.br

Ricardo de Vasconcelos Salvo

Federal Technologic University of Parana.
Av. Alberto Carazzai, 1640, Cornelio Procopio, Parana, Brazil.
rvsalvo@hotmail.com

Abstract. Numerical simulations in confined rotating flows were performed in this work, in order to verify and characterize the formation of the vortex breakdown phenomenon. Cylindrical and conical-cylindrical geometries, both closed, were used in simulations. The rotating flow is induced by the bottom wall, which rotates at constant angular velocity. First, the numerical results were compared to experimental results available in references, aiming to verify the capacity of the computational code to predict the vortex breakdown phenomenon. Further, several simulations varying the parameters which govern the characteristics of the flows analyzed in this work, i.e. the Reynolds number and the aspect ratio were performed. In these simulations, the transitional limit and the limit of the vortex breakdown formation were verified. Steady and transient cases, with and without turbulence modeling, were simulated. In general, some aspects of the process of vortex breakdown in conical-cylindrical geometries were observed to be different from that in cylinders.

Keywords: Vortex Breakdown, Transitional Flows, CFD.

1. INTRODUCTION

Rotating flows occur in various natural phenomena, like in hurricanes and tornados. In industry, it is often used in combustion chambers, turbines, pumps, and cyclone separators. As in other types of flow, rotating flow displays specific features. A typical phenomenon in rotating flow is the vortex breakdown, which can be defined as an abrupt change in flow direction in certain points along the rotation axis, creating one or more recirculation zones with stagnation points, spiral or helical structures. The first scientific record of the vortex breakdown was made by Peckham e Atkinson (1957). By running experiments with delta wings, they observed the breakdown in the leading edge vortices at high angles of attack. The phenomenon was later confirmed in other cases, as in confined rotating flow and vortex tubes. Different forms of breakdown were observed. Sarpkaya (1971) identified three forms of vortex breakdown: axisymmetric bubble, spiral and double helix.

In industry, vortex breakdown can be observed in a number of situations, and it may have a positive influence, like in swirl combustors, in which it acts as an efficient mixer for the combustion process. On the other hand, in industrial cyclones, the bubble can retain particles in the recirculation zones, thus hindering the separation process.

The objective of this paper is to carry out numerical simulations in flows similar to that in cyclones and combustion chambers, in order to assess and characterize the formation of vortex breakdown phenomenon. Three geometries were investigated, namely a cylinder, a cylinder coupled to a truncated cone and a truncated cone coupled to a cylinder. In all the geometries the bottom wall is rotating, and the other walls are nonmoving with a no-slip boundary condition.

The features of rotating flows confined in cylindrical and conical-cylindrical geometries are similar. The rotating bottom wall acts as a pump, driving the fluid centrifugally to the side walls through the Ekman layer. In this layer, the Coriolis force is greater than the viscous force, and the swirling flow generates a depression zone in center. In the side walls, the flow is driven towards the top wall by the Stewartson layer. In this situation, the viscous force is predominant. In the top wall, the flow moves inward in the Bödewadt layer and down in direction to the Ekman layer, originating the central vortex.

2. MATHEMATICAL MODELS

Martins, D. A. M., Souza, F. J. and Salvo, R. V.
Numerical Simulations of the Vortex Breakdown Phenomenon.

The filtered Navier-Stokes equations for an incompressible flow and Newtonian fluid, are solved by the finite volume method in unstructured meshes. The equations can be describe by the follow form:

$$\frac{\partial \bar{u}_i}{\partial x_i} = 0 \quad (1)$$

$$\frac{\partial \bar{u}_i}{\partial t} + \frac{\partial (\bar{u}_i \bar{u}_j)}{\partial x_j} = -\frac{1}{\rho} \frac{\partial \bar{p}^*}{\partial x_i} + \frac{\partial}{\partial x_j} \left[(\nu + \nu_t) \left(\frac{\partial \bar{u}_i}{\partial x_j} + \frac{\partial \bar{u}_j}{\partial x_i} \right) \right] \quad (2)$$

Transient and steady cases were simulated. In steady cases, no turbulence model was used. The dynamic Smagorinsky model was used in turbulence modeling in the transient cases. The eddy viscosity is represented by Eq. (3) (Germano et al., 1991).

$$\nu_t = C \bar{\Delta}^2 \bar{S} \quad (3)$$

The model coefficient C is modeled as follows:

$$C = \frac{1}{2} \left(\frac{L_{ij} M_{ij}}{M_{ij}^2} \right) \quad (4)$$

where L_{ij} is the Leonard tensor and M_{ij} is the subgrid Reynolds tensor.

$$L_{ij} = \bar{u}_i \bar{u}_j - \bar{u}_i \bar{u}_j \quad (5)$$

$$M_{ij} = \left(\tilde{\Delta}^2 \left| \tilde{S} \right| \tilde{S}_{ij} - \bar{\Delta}^2 \left| \bar{S} \right| \bar{S}_{ij} \right) \quad (6)$$

Δ is the grid length, S_{ij} is the strain-rate tensor, $(\bar{\quad})$ denotes the grid filter, and $(\tilde{\quad})$ denotes the test filter. Normally $\tilde{\Delta}/\bar{\Delta} = 2$.

The simulations were run with the computational code UNSCYFL3D (Unsteady Cyclone Flow 3 D) developed in MFlab (Laboratório de Mecânica dos Fluidos). The solution of the pressure-velocity coupling was realized through the SIMPLE algorithm (Semi-Implicit Method for Pressure-Linked Equation). The second-order central differencing scheme was used for spatial discretizations. For the transient simulations, the three-time level method was used for the time advancement.

3. RESULTS

To verify if the second order methods used in this work can evidence the vortex breakdown, the cases experimented by Escudier (1984) were simulated. Those experiments were done in a closed cylindrical container with a rotating endwall, varying the aspect ratio H/R and Reynolds number $Re = \Omega R^2/\nu$, H being the cylinder length, R its radius, Ω the angular velocity of the endwall and ν the kinematic viscosity of the contained fluid. The streamlines were photographed in the middle plan along the axial axis. A summary of cases simulated are shown in Tab. 1. Figs. 1 and 2 show a comparison between the experimental and numerical streamlines, for cases 1 and 2, respectively.

Table 1. Simulation parameters.

| Case | Geometry | Regime | Turbulence Model | Re | H/R | Mesh |
|------|----------|-----------|------------------|------|-------|---------|
| 1 | Cylinder | Steady | No model | 1854 | 2.0 | 891,000 |
| 2 | Cylinder | Transient | Dynamic | 2752 | 3.25 | 690,000 |
| 3 | Cylinder | Steady | No model | 1002 | 2.0 | 891,000 |
| 4 | Cylinder | Steady | No model | 1492 | 2.0 | 891,000 |
| 5 | Cylinder | Steady | No model | 2494 | 2.5 | 620,000 |

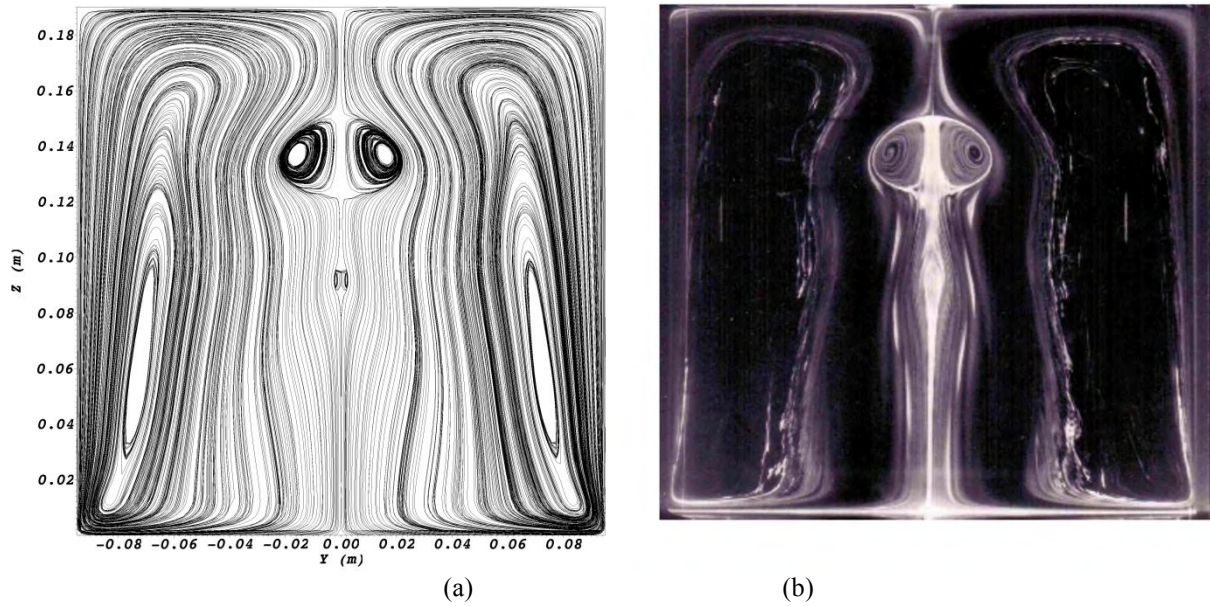


Figure 1. Streamlines obtained numerically (a) and experimentally by Escudier (1984) (b), for case 1.

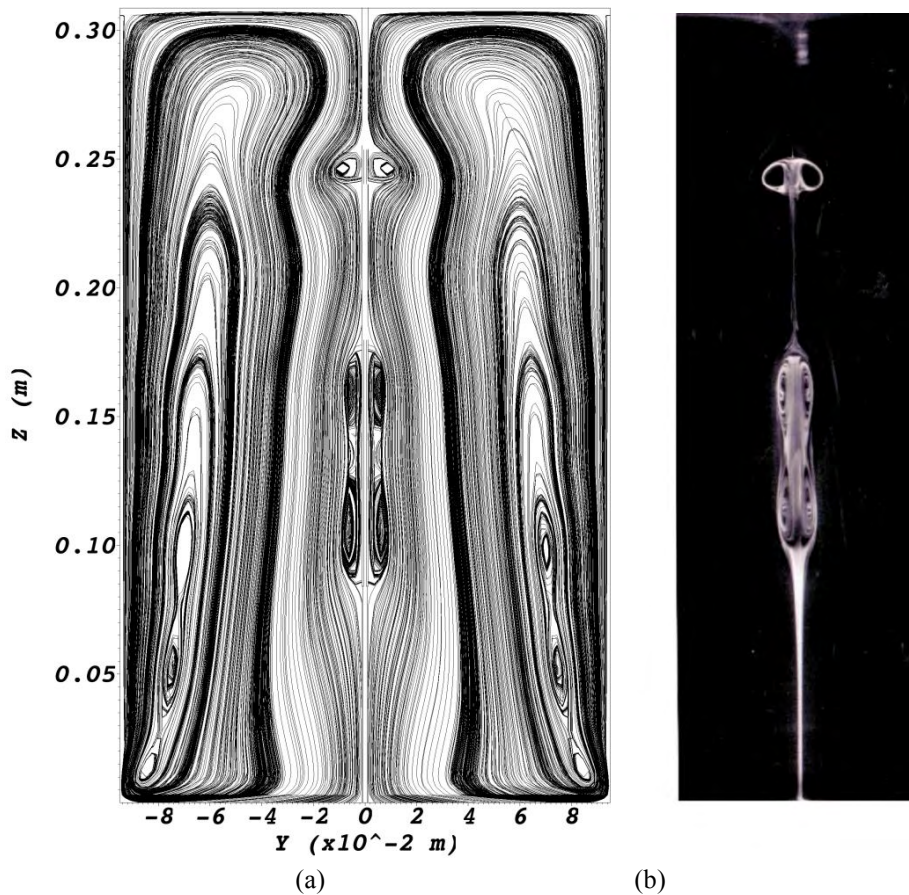


Figure 2. Streamlines obtained numerically (a) and experimentally by Escudier (1984) (b), for case 2.

It can be seen the numerical results resemble the experimental ones, ensuring the capacity of the code to predict the vortex breakdown. Other four cases were simulated and the agreement was good as well.

Cases with increasing Reynolds numbers in cylinder were simulated, for $H/R=2.0$. The simulation parameters are shown in Tab. 2.

Martins, D. A. M., Souza, F. J. and Salvo, R. V.
 Numerical Simulations of the Vortex Breakdown Phenomenon.

Table 2. Simulation parameters.

| Case | Geometry | Regime | Turbulence Model | Re | H/R | Mesh |
|------|----------|--------|------------------|------|-------|---------|
| 6 | Cylinder | Steady | No model | 1000 | 2.0 | 891,000 |
| 7 | Cylinder | Steady | No model | 1100 | 2.0 | 891,000 |
| 8 | Cylinder | Steady | No model | 1200 | 2.0 | 891,000 |
| 9 | Cylinder | Steady | No model | 1300 | 2.0 | 891,000 |
| 10 | Cylinder | Steady | No model | 1400 | 2.0 | 891,000 |
| 11 | Cylinder | Steady | No model | 1500 | 2.0 | 891,000 |

Streamlines in an axial plan were plotted, which character the process of the vortex breakdown formation.

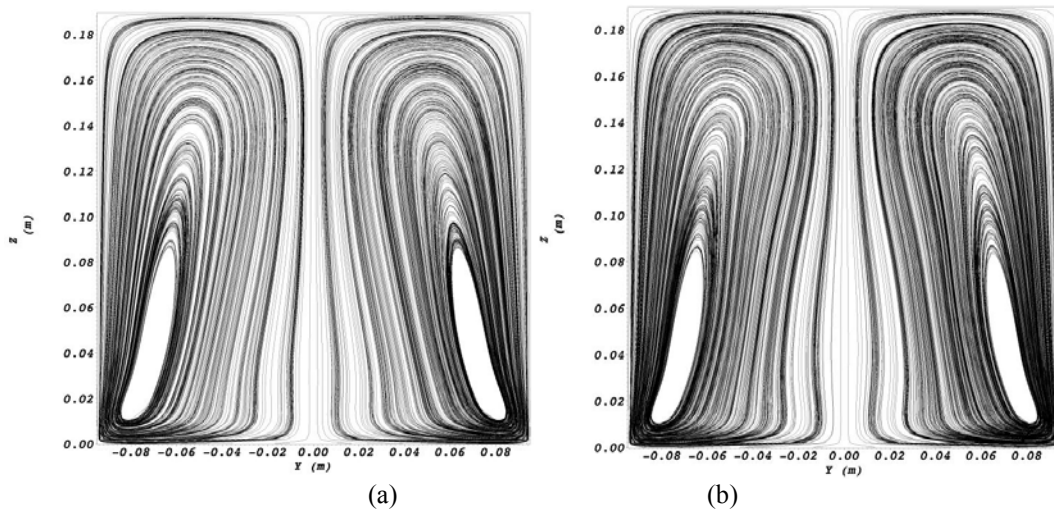


Figure 3. Streamlines for case 6 (a) and case 7 (b).

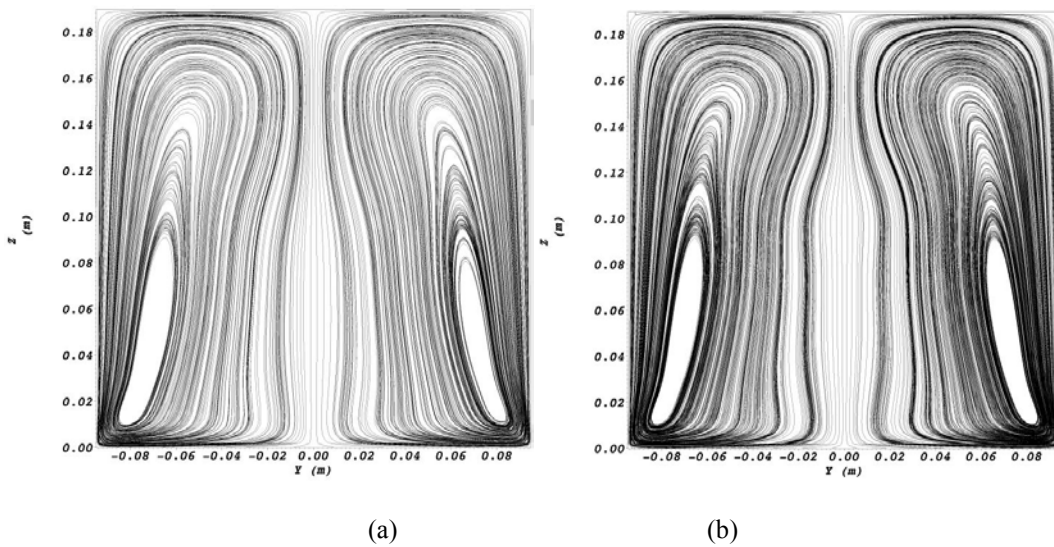


Figure 4. Streamlines for case 8 (a) and case 9 (b).

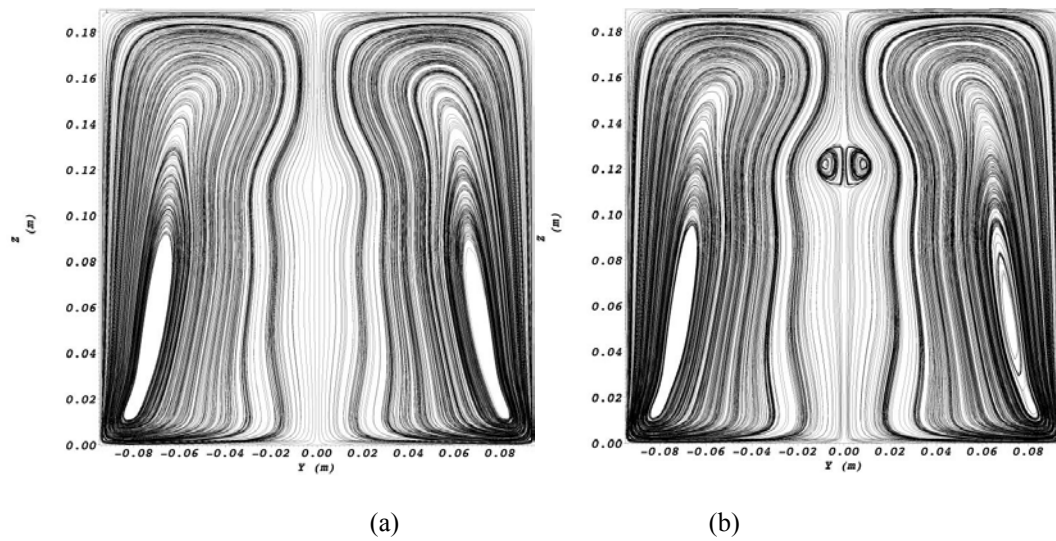


Figure 5. Streamlines for case 10 (a) and case 11 (b).

The evolution of central vortex until the formation of the vortex breakdown was observed with increasing Reynolds number. The central vortex core expands, first near the bottom wall region, and later in a superior region forming an hour-glass structure. The axisymmetric bubble appears at $Re = 1500$. Contours of negative axial velocity, which better evidence the central vortex are displayed in Figs 6 to 10.

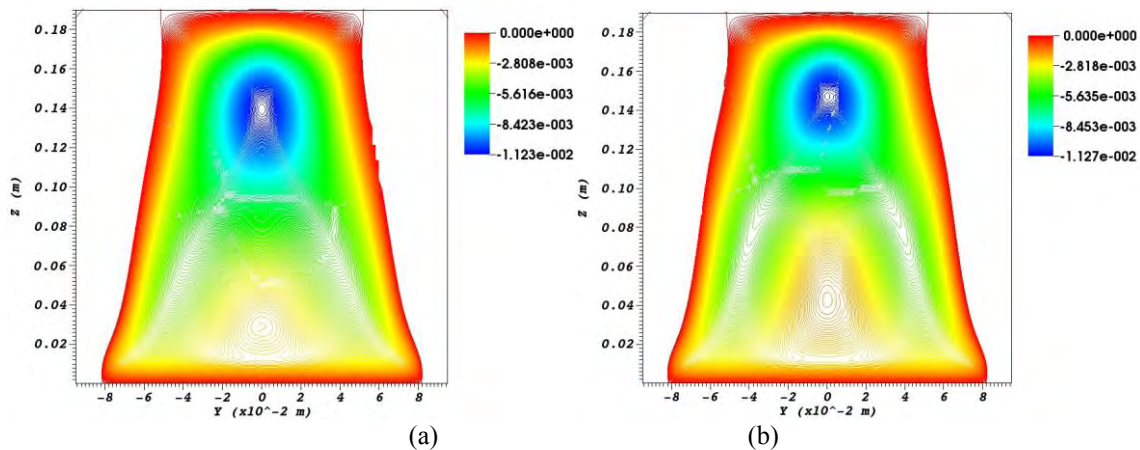


Figure 6. Contour of negative axial velocity for case 6 (a) and case 7 (b).

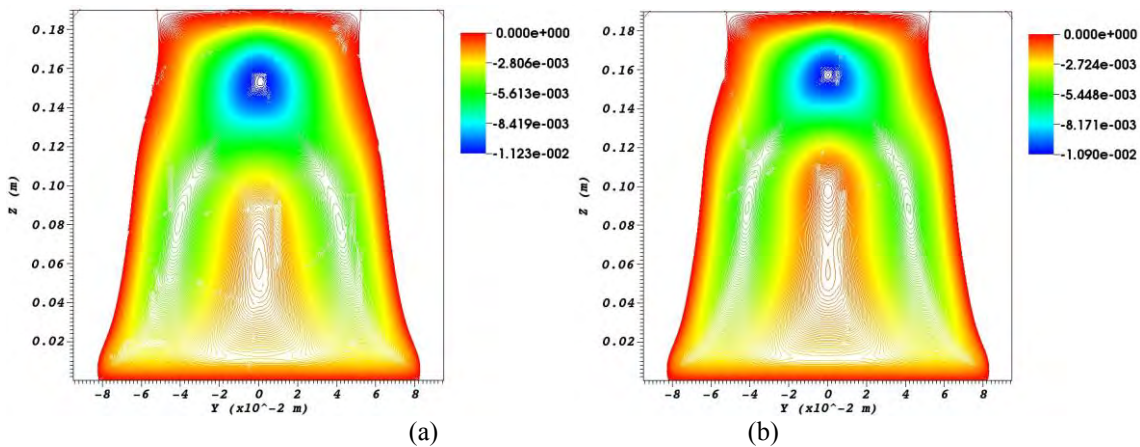


Figure 7. Contour of negative axial velocity for case 8 (a) and case 9 (b).

Martins, D. A. M., Souza, F. J. and Salvo, R. V.
 Numerical Simulations of the Vortex Breakdown Phenomenon.

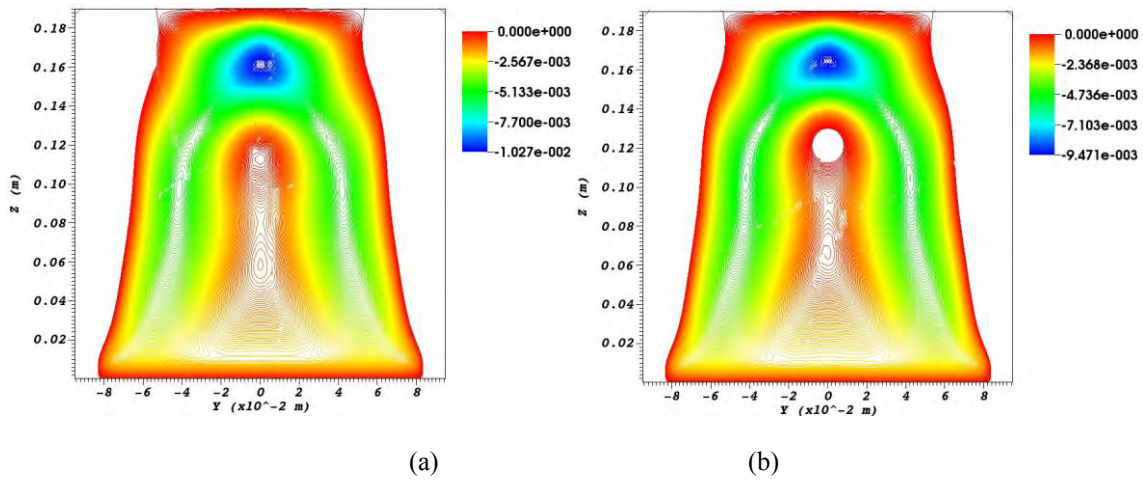


Figure 8. Contour of negative axial velocity for case 10 (a) and case 11 (b).

By increasing the Reynolds number, the central vortex increases in diameter and the axial flow decelerates, originating the vortex breakdown. The negative values of Q-criterion contour, illustrates the behavior of the Stewartson and Bödewadt layers.

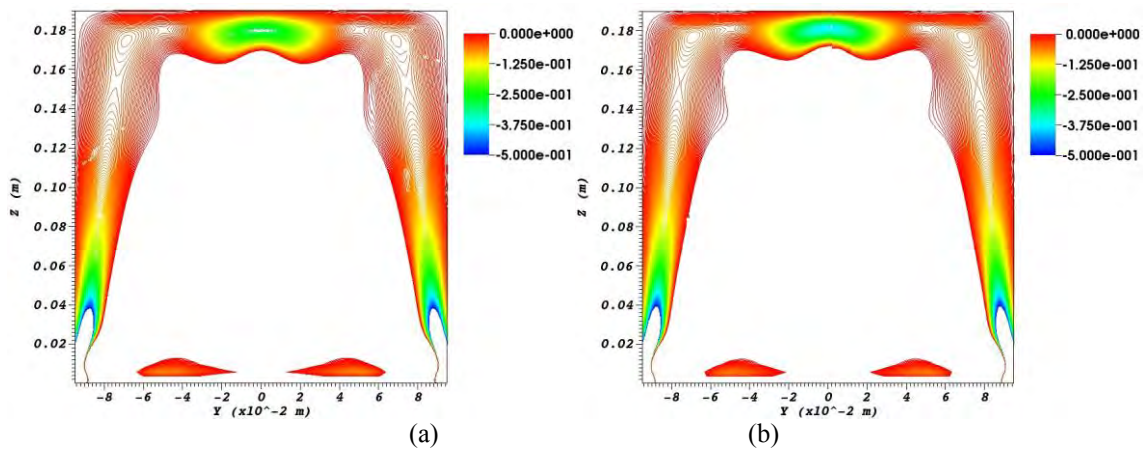


Figure 9. Contour of negative Q-criterion for case 6 (a) and case 7 (b).

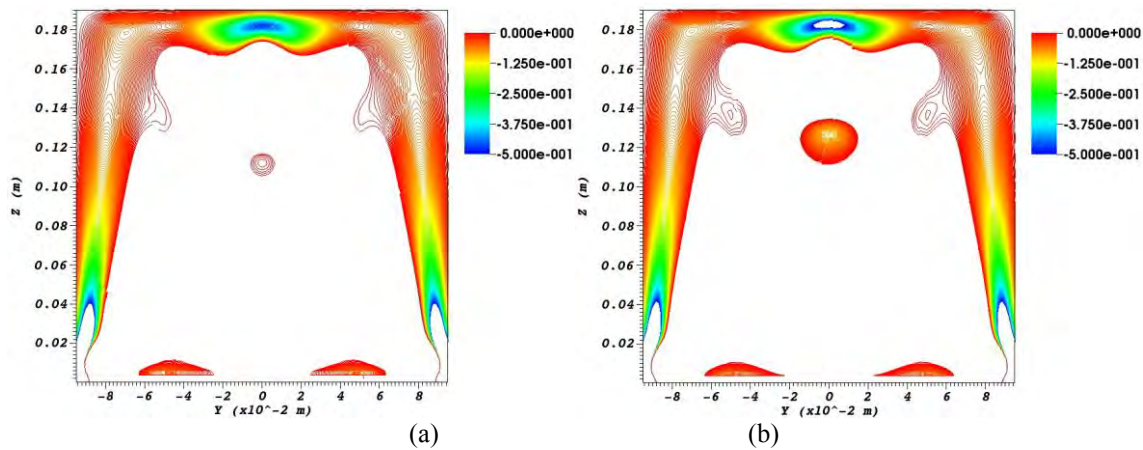


Figure 10. Contour of negative Q-criterion for case 8 (a) and case 9 (b).

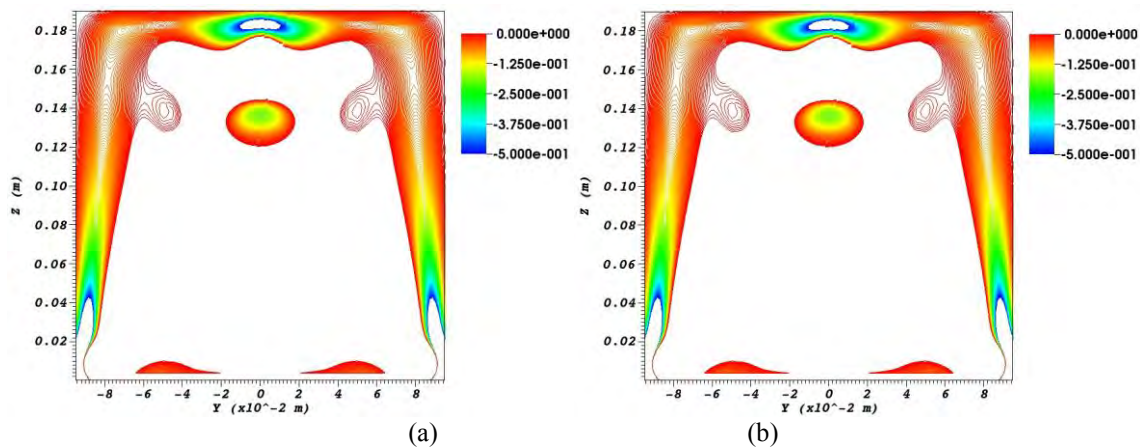
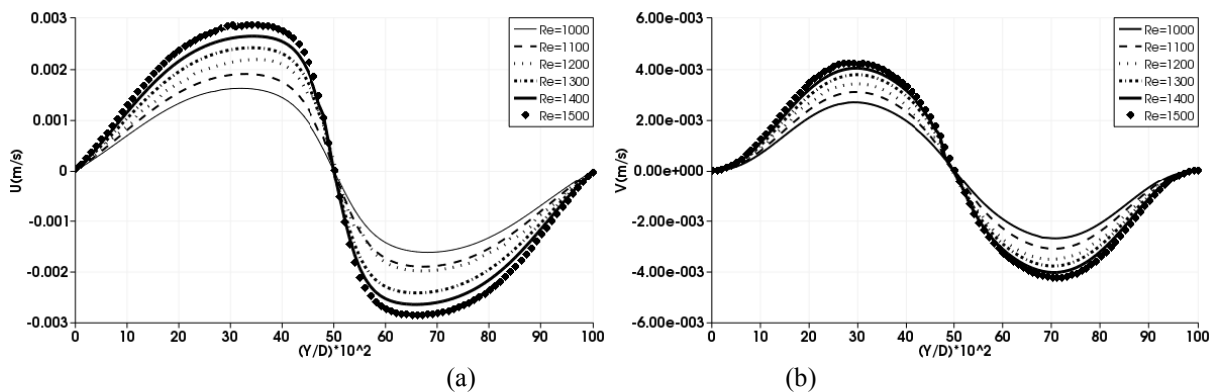
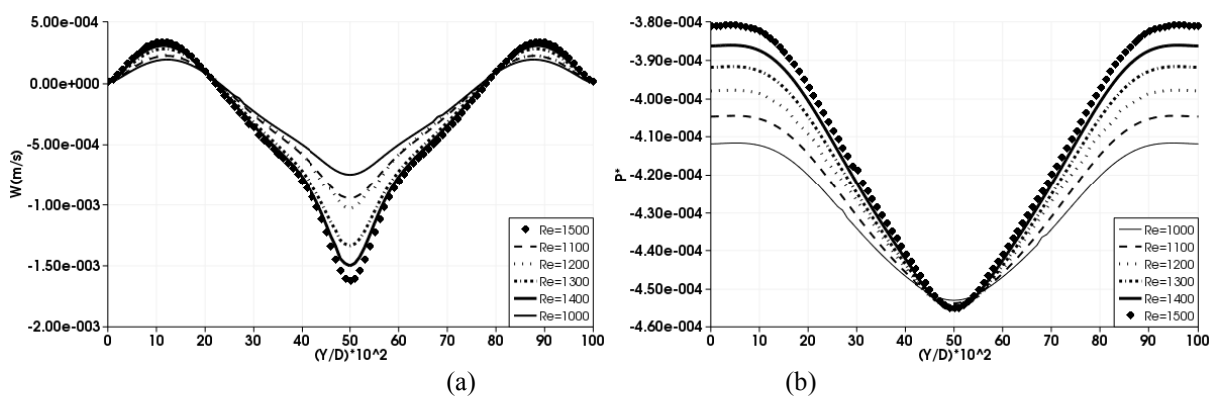


Figure 11. Contour of negative Q-criterion for case 10 (a) and case 11 (b).

The Q-criterion represents the balance between the vorticity rate and the strain rate. Negative values consider only the strain rate, excluding the vorticity field. Based on the strain rate, it is possible to observe that the Stewartson and Bödewadt layers decrease in thickness with increasing Reynolds number.

Radial profiles of velocities and pressure are shown in Figs. 12 and 13. It can be observed that the region near the top wall is the most affected with the increasing of the Reynolds number.

Figure 12. Radial velocity (a) and tangential velocity (b) profiles at $H/R=1.95$ Figure 13. Axial velocity (a) and relative pressure (b) profiles at $H/R=1.95$.

By increasing the Reynolds number, the swirl level close to the Bödewadt layer (near the top wall) increases also. This creates a strong axial pressure gradient, which decelerates the axial flow. Depending on the pressure gradient magnitude, flow reversal occurs, forming a quasi-stagnant recirculation zone, or vortex breakdown.

In order to assess that the causes of vortex breakdown formation are the same in all geometries studied in this paper, the flow in conical-cylindrical cavities were simulated. The simulation parameters are shown in Tab. 3.

Martins, D. A. M., Souza, F. J. and Salvo, R. V.
Numerical Simulations of the Vortex Breakdown Phenomenon.

Table 3. Simulation parameters.

| Case | Geometry | Regime | Turbulence Model | Re | H/R | Mesh |
|------|---------------|--------|------------------|------|-------|---------|
| 12 | Cylinder | Steady | No model | 1500 | 2.0 | 891,000 |
| 13 | Cylinder-cone | Steady | No model | 1500 | 2.0 | 891,000 |
| 14 | Cone-Cylinder | Steady | No model | 1500 | 2.0 | 891,000 |

Streamlines in the central axial plan are displayed in Fig. 14. It can be observed that the vortex breakdown occurs in the cylinder, and a small structure appears in the cone-cylinder. No structure was observed in the cylinder-cone at this Reynolds number.

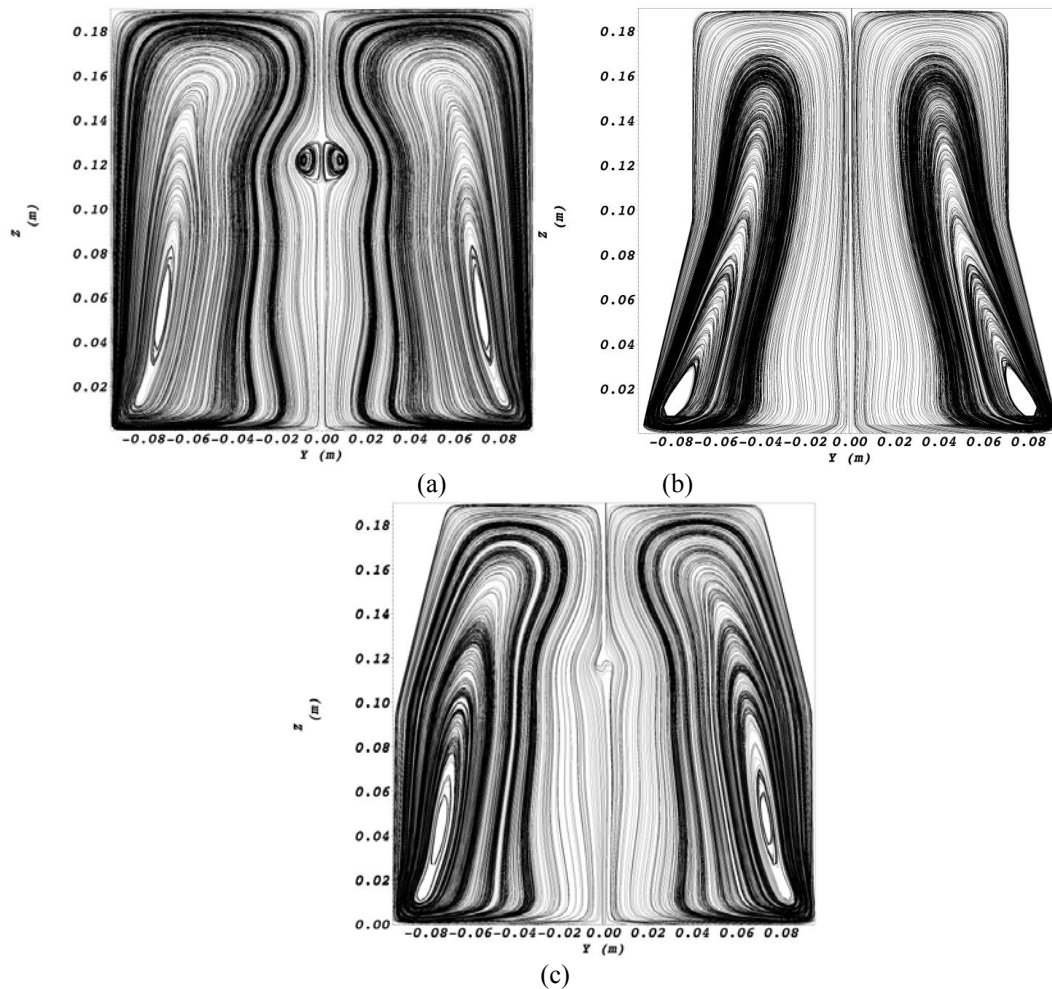


Figure 14. Streamlines for cylinder (a), cylinder-cone (b) cone-cylinder (c). $H/R=2.0$ and $Re=1,500$.

Radial profiles for velocity components and relative pressure are plotted for cases 12, 13 and 14 in Figs. 15 ad 16.

22nd International Congress of Mechanical Engineering (COBEM 2013)
November 3-7, 2013, Ribeirão Preto, SP, Brazil

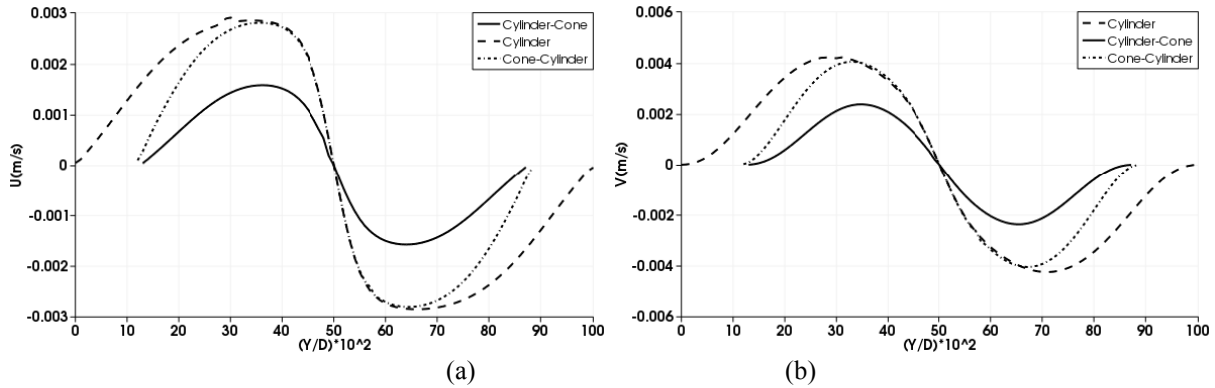


Figure 15. Radial velocity (a) and tangential velocity (b) profiles at $H/R=1.95$

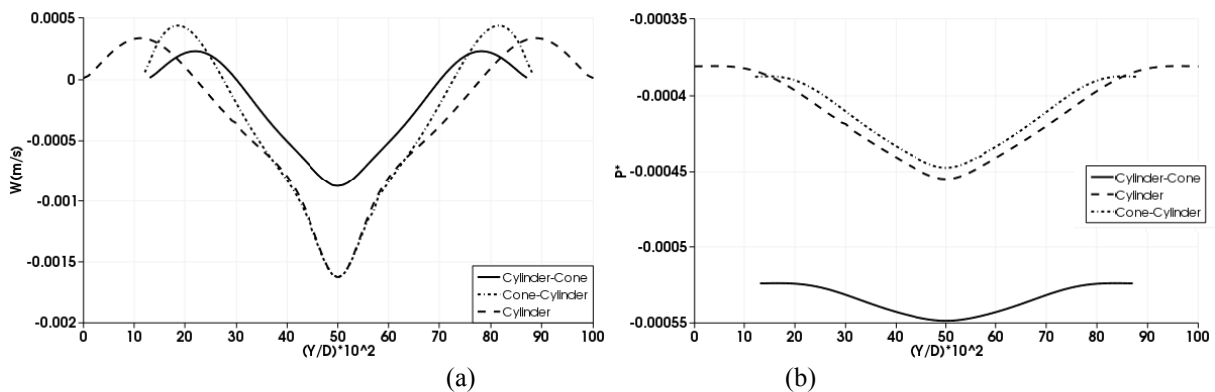


Figure 16. Axial velocity (a) and relative pressure (b) profiles at $H/R=1.95$.

By observing the profiles above, it is noticed that the factor which causes the vortex breakdown in the cases analyzed in this work is the depression created by swirl next to the Bödewadt layer. This is confirmed by the cases cylinder and cone-cylinder, in which there is evidence of vortex breakdown. In these cases, the angular velocity is greater and the pressure gradient is stronger.

In order to check the stability limits of the cases investigated, higher Reynolds numbers were simulated. In these computations, interesting effects in the boundary layers and in the vortex breakdown were observed. For the cylinder-cone with $Re=3750$ and $H/R=2.5$ the flow remains steady, but the Stewartson layer (near the sidewall) displays some instabilities. Ring vortices are formed in the Stewartson layer, which travel upward in a spiral movement, characterizing the beginning of transitional regime. This is shown by the iso-surface of Q -criterion of Fig. 17(b). Another interesting effect is the formation of the lower vortex breakdown earlier than the upper one, as shown in Fig. 17(a). This is in contrast with the experiments of Escudier 1984, in which the superior breakdown appears earlier for ratios $H/R \leq 3.25$.

Martins, D. A. M., Souza, F. J. and Salvo, R. V.
 Numerical Simulations of the Vortex Breakdown Phenomenon.

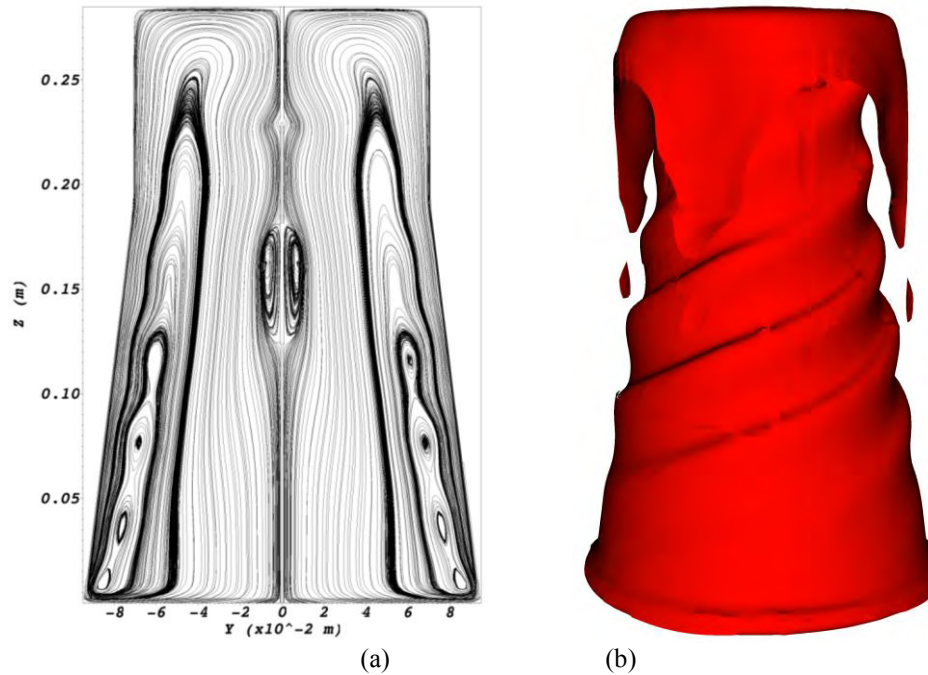


Figure 17. Streamlines (a) and iso-surface (b), obtained with cylinder-cone for $Re=3,750$ and $H/R=2.5$.

For $Re=3,000$ and $H/R=2.0$, in the cone-cylinder case, the axisymmetric bubble is distorted due to viscous effects. It acts as a separated body, experiencing the stresses imposed by the flow. Figure 18(a) shows these effects along with the streamlines, and figure 18(b) shows the contours of Q-criterion in a middle plan along the cylinder axis.

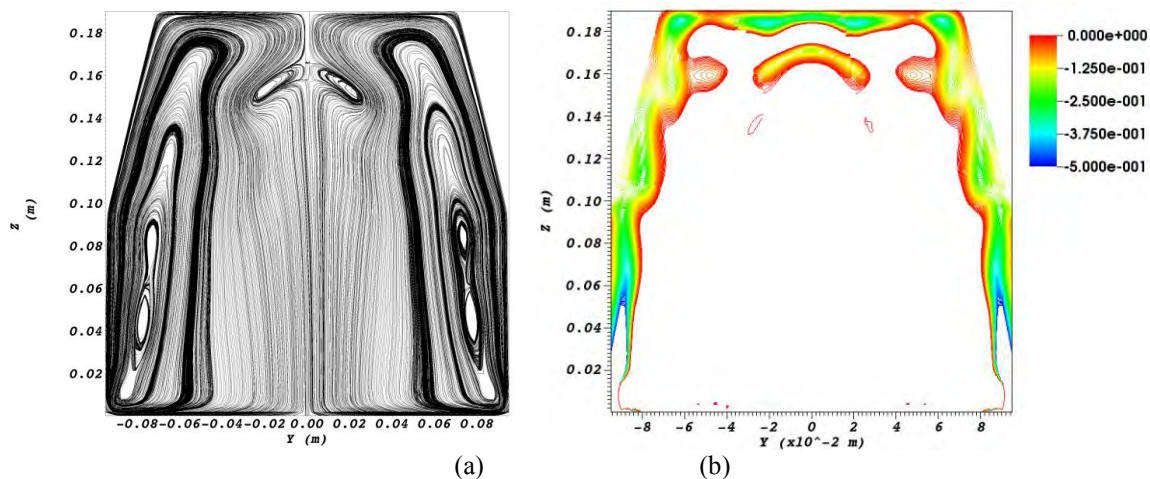


Figure 18. Streamlines (a) and Q-criterion contour (b), obtained with cone- cylinder, for $Re=3,000$ and $H/R=2.0$

4. CONCLUSION

To solve rotating flows in conical-cylindrical cavities, the Navier-Stokes equations for incompressible flow were used. The equations were discretized by the finite volume method in unstructured meshes, and second order methods were used for temporal and spatial derivatives.

The ability to predict the vortex breakdown phenomenon with second order methods was confirmed, provided that the mesh is sufficiently refined. Methods of higher order can possibly predict the vortex breakdown phenomenon with less refined meshes

In all geometries simulated, it was observed that the factor causing the vortex breakdown is the depression created by swirl in the proximity of the Bödewadt layer (near the top wall). This depression decelerates the axial flow, inducing the reverse flow and forming a quasi-stagnant region.

22nd International Congress of Mechanical Engineering (COBEM 2013)
November 3-7, 2013, Ribeirão Preto, SP, Brazil

It was also observed that the first instabilities appear in Stewartson layer (near the side wall), with vortex rings which travel in a spiral motion to the topwall. For relatively high Reynolds numbers, the axisymmetric breakdown deforms due to viscous effects. It acts as a separate body, experiencing the stresses imposed by the flow.

5. ACKNOWLEDGEMENTS

The authors thank Professor Marcel Escudier, University of Liverpool, for sending us the experimental results, CNPq and CAPES/PROEX for the financial support.

6. ACKNOWLEDGEMENTS

Escudier, M. P., 1984. "Observations of the flow produced in a cylindrical container by a rotating end wall".

Experiments in Fluids, Vol. 2, pp. 179-186.

Germano, M., Piomelli, U., Moin, P. and Cabot, W. H., 1991. "A dynamic subgrid-scale eddy viscosity model", Physics Fluids, Vol. 3, no. 7, 1760-1765.

Peckham, D. H. e Atkinson, S. A., 1957. "Preliminary results of low speed wind tunnel tests on a Gothic wind of aspect ratio 1.0", Aero. Res. Council Current Paper, no. 508.

Sarpkaya, T., 1971. "On stationary and travelling vortex breakdowns", Journal of Fluid Mechanics, Vol. 45, pp. 545-559.